Acta Crystallographica Section D
Biological Crystallography
ISSN 0907-4449

Location and conformation of pantothenate and its derivatives in *Mycobacterium tuberculosis* pantothenate kinase: insights into enzyme action

Bhaskar Chetnani,[a] Parimal Kumar,[a] K. V. Abhinav,[a] Manmohan Chhibber,[a] A. Surolia[a,b] and M. Vijayan[a]*

[a]Molecular Biophysics Unit, Indian Institute of Science, Bangalore 560 012, India, and [b]National Institute of Immunology, Aruna Asaf Ali Marg, New Delhi 110 067, India

Correspondence e-mail: mv@mbu.iisc.ernet.in

Received 21 March 2011
Accepted 22 June 2011

PDB References: *Mt*PanK, binary complex with pantothenate, 3avo; binary complex with pantothenol, 3avp; binary complex with N9-Pan, 3avq.

Previous studies of complexes of *Mycobacterium tuberculosis* PanK (*Mt*PanK) with nucleotide diphosphates and non-hydrolysable analogues of nucleoside triphosphates in the presence or the absence of pantothenate established that the enzyme has dual specificity for ATP and GTP, revealed the unusual movement of ligands during enzyme action and provided information on the effect of pantothenate on the location and conformation of the nucleotides at the beginning and the end of enzyme action. The X-ray analyses of the binary complexes of *Mt*PanK with pantothenate, pantothenol and *N*-nonylpantothenamide reported here demonstrate that in the absence of nucleotide these ligands occupy, with a somewhat open conformation, a location similar to that occupied by phosphopantothenate in the 'end' complexes, which differs distinctly from the location of pantothenate in the closed conformation in the ternary 'initiation' complexes. The conformation and the location of the nucleotide were also different in the initiation and end complexes. An invariant arginine appears to play a critical role in the movement of ligands that takes place during enzyme action. The work presented here completes the description of the locations and conformations of nucleoside diphosphates and triphosphates and pantothenate in different binary and ternary complexes, and suggests a structural rationale for the movement of ligands during enzyme action. The present investigation also suggests that *N*-alkylpantothenamides could be phosphorylated by the enzyme in the same manner as pantothenate.

1. Introduction

The first step in the biosynthesis of coenzyme A (CoA), namely the ATP-mediated phosphorylation of pantothenate (vitamin B_5), is catalyzed by the enzyme pantothenate kinase (PanK; Leonardi *et al.*, 2005). Three types of PanK are found in bacteria, of which type I PanK, often referred to simply as PanK, is the best characterized. In addition to its importance as an enzyme involved in the biosynthesis of an essential coenzyme, PanK is also considered to be a possible drug target on account of the difference between the human and the bacterial enzymes (Spry *et al.*, 2008). The structure and interactions of bacterial PanK were first characterized in detail through X-ray analysis of the complexes of the *Escherichia coli* enzyme (*Ec*PanK) with CoA (a feedback inhibitor), with AMPPNP (a nonhydrolysable analogue of ATP), and with ADP and pantothenate (Yun *et al.*, 2000; Ivey *et al.*, 2004). *Ec*PanK exhibits considerable structural plasticity. Its structure also exhibits significant differences between the CoA complex

and the other two complexes. Also, CoA and AMPPNP/ADP interact with the enzyme in substantially different ways, although their phosphate groups all interact with the P-loop (Yun *et al.*, 2000).

Subsequently, we carried out detailed structural investigations of the enzyme from *Mycobacterium tuberculosis* (*Mt*PanK) and its complexes as part of a long-range programme on the structural biology of mycobacterial proteins (Vijayan, 2005; Das *et al.*, 2006; Krishna *et al.*, 2007; Selvaraj *et al.*, 2007; Roy *et al.*, 2008; Prabu *et al.*, 2009). Initially, the structure of the binary complex of *Mt*PanK with CoA was analyzed (Das *et al.*, 2006). The structure of the subunit and its interactions with CoA were essentially the same as those in *Ec*PanK; the comparatively small differences between the two enzymes were primarily in the association between the two subunits. The structures subsequently analyzed included the ternary complexes with another nonhydrolysable ATP analogue AMPPCP and pantothenate (the initiation complex), with ADP and phosphopantothenate resulting from phosphorylation of pantothenate by ATP in the crystal (the end complex) and with ADP and pantothenate, as well as the binary complexes with ADP and AMPPCP (Chetnani *et al.*, 2009, 2010). The results suggested a possible dual specificity of the enzyme for ATP and GTP, which was confirmed through kinetic measurements of enzyme activity. This led to detailed X-ray analysis of the type of complexes studied earlier with GMPPCP instead of AMPPCP and GDP instead of ADP (Chetnani *et al.*, 2010). A detailed examination of the complexes involving adenine and guanine nucleotides and solution studies resulted in a comprehensive picture of the structure, interactions and enzyme activity of *Mt*PanK, with special reference to the differences between the homologous *Ec*PanK and *Mt*PanK.

The investigations referred to above led to a clear enunciation of the structural basis for the dual specificity of *Mt*PanK as distinct from the specificity of *Ec*PanK for ATP. The structural plasticity of *Ec*PanK that was observed on binding to AMPPNP or ADP, which is not exhibited by *Mt*PanK, could be explained in terms of changes in the local structure resulting from amino-acid substitutions (Chetnani *et al.*, 2009). Unlike in the case of *Ec*PanK, the location and conformation of the ligands undergo substantial changes during the action of *Mt*PanK. The nucleoside diphosphate (NDP) and the nucleoside triphosphate (NTP) bind with an extended conformation at the same site, as shown by their binary complexes with *Mt*PanK. In the presence of pantothenate, as in the initiation complexes, the NTP has a closed conformation and an altered location. However, the effect of the nucleotide on the conformation and the location of pantothenate has yet to be elucidated as the natural location of the ligand in *Mt*PanK is not known. We sought to fill this lacuna through X-ray analysis of the binary complexes of *Mt*PanK with pantothenate and two of its derivatives, namely pantothenol and *N*-nonylpantothenamide (N9-Pan). Pantothenol is also a substrate of *Mt*PanK, but the product 4′-phosphopantothenol competitively inhibits the utilization of 4′-phosphopantothenate by *CoaBC*, which follows *Mt*PanK in the CoA-biosynthesis pathway (Kumar *et al.*, 2007). N9-Pan belongs to the *N*-alkylpantothenamide class of inhibitors such as N5-Pan. N5-Pan can be effectively phosphorylated by *Ec*PanK and the product of the reaction can subsequently be converted by the downstream enzymes of the CoA-biosynthesis pathway (*CoaD* and *CoaE*) into an inactive CoA derivative which, when incorporated into an acyl carrier protein (ACP), results in inhibition of fatty-acid metabolism (Strauss & Begley, 2002; Zhang *et al.*, 2004). However, it has recently been reported that the enzyme ACP phosphodiesterase readily hydrolyses the inactive CoA derivative and that N5-Pan inhibits CoA synthesis, although it is not clear at which step in the synthetic pathway inhibition occurs (Thomas & Cronan, 2010). It has been suggested that the mode of action of pantothenamide analogues could be through a combination of the inhibition of CoA synthesis and fatty-acid synthesis and perhaps enzymes that utilize CoA or acetyl-CoA. In any case, the inhibitory action of pantothenamides merits further investigation. In this context, it may be noted that the N9-Pan–*Mt*PanK complex reported here is the first experimentally determined structure of a PanK with a bound pantothenamide. In addition to providing information on the natural locations and conformations of bound pantothenate and its analogues, the three crystal structures reported here complete the picture of the location of ligands in the initial and the final stages of enzyme action and lead to further insights into the structural rationale for their movement during catalysis.

2. Materials and methods

2.1. Synthesis of N9-Pan

Synthesis of N9-Pan was carried out by a protocol similar to that described by Strauss and Begley for the synthesis of N5-Pan (Strauss & Begley, 2002). Sodium pantothenate (1.0 g, 4.1 mmol) was dissolved in deionized water (5.0 ml) and the solution was passed through an Amberlite IR-120 (H^+) column. The column was washed with deionized water (2 × 5.0 ml) and the combined aqueous solutions were lyophilized. The viscous oil of pantothenic acid obtained was further dissolved in dry dimethylformamide (10 ml) and nonylamine (0.9 ml, 5.0 mmol). Diphenylphosphoryl azide (1.1 ml, 5.0 mmol) was added and the solution was cooled to 273 K. Triethylamine (0.7 ml, 5.0 mmol) was added and the solution was stirred at 273 K for 2 h followed by stirring at room temperature overnight. The solvent was evaporated under vacuum using a rotary evaporator and a water bath. The viscous oil thus obtained was purified using column chromatography on silica gel (60–120 mesh) with 95:5 CH_2Cl_2:methanol as the solvent. Thin-layer chromatography (TLC) was used to detect fractions containing N9-Pan. All fractions containing the product were pooled together and evaporated under vacuum using a rotary evaporator and water bath. The white crystalline powder obtained was characterized using ^{1}H and ^{13}C NMR and mass spectrometry. ^{1}H NMR (400 MHz, $CDCl_3$): δ 0.84–0.90 (m, 6H), 0.98 (s, 3H), 1.24 (m, 12H), 1.46

(m, 2H), 2.41 (t, 6.0 Hz, 2H), 3.18 (dd, 6.8 Hz, 2H), 3.46–3.60 (m, 4H), 3.89 (bs, 1H), 3.98 (d, 1H), 4.44 (d, 1H), 6.22 (t, 1H), 7.48 (t, 1H). ^{13}C NMR (75 MHz, $CDCl_3$): δ 13.98, 20.41, 21.00, 22.53 (2C), 26.88, 29.15, 29.22, 29.29, 29.40, 31.73, 35.32, 35.70, 39.16, 39.65, 70.49, 171.51, 174.19. Exact mass calculated for $C_{18}H_{36}N_2O_4$ = 344.3; mass obtained from electrospray-MS m/z = 345.2 $[M + H]^+$, 367.3 $[M + Na]^+$, 383.0 $[M + K]^+$. All chemicals used in the synthesis were obtained from Sigma–Aldrich. The ^{1}H NMR and ^{13}C NMR spectra were measured on Bruker 400 MHz and Jeol 300 MHz instruments, respectively. ESI–MS analyses were performed on a Bruker Daltonics Esquire 3000 Plus ion-trap mass spectrometer.

2.2. Phosphorylation of N9-Pan by *Mt*PanK

The ability of *Mt*PanK to phosphorylate N9-Pan was demonstrated by preparing a series of reaction mixtures (25 µl) that contained a progressively increasing concentration of N9-Pan (0–1.6 m*M*) together with 2.5 mg *Mt*PanK, 10 m*M* $MgCl_2$, 5 m*M* ATP, 68 n*M* [γ-^{32}P]-ATP and 2%(*v*/*v*) DMSO in 25 m*M* Tris–HCl pH 8.0. The reaction mixtures were incubated at 310 K for 10 min and were heated at 353 K for 5 min to stop the reaction. The reaction mixture was spun at 10 000 rev min^{-1} for 10 min and 5 µl of the supernatant was loaded onto a silica gel 60 TLC plate. The plate was developed with a 5:2:4(*v*:*v*:*v*) butanol:acetic acid:water solvent system and the separated radiolabelled components were visualized by autoradiography using a Fujifilm phosphorimager.

2.3. Cloning, expression, purification and crystallization

Recombinant *Mt*PanK was cloned, expressed and purified and the protein-bound CoA was removed using a previously described protocol (Chetnani *et al.*, 2009, 2010). Diffraction-quality crystals of *Mt*PanK were obtained using a precipitant solution consisting of 1.4–1.8 *M* trisodium citrate, 0.05–0.1 *M* sodium acetate and 10% glycerol at pH 6.5 (Chetnani *et al.*, 2009, 2010). The crystals were cryoprotected by increasing the glycerol concentration from 10%(*v*/*v*) to 40%(*v*/*v*) over a period of 16 h. To obtain the different *Mt*PanK complexes, 0.5 *M* solutions of pantothenate and pantothenol were prepared in protein buffer and 1 µl of each was added to the drop containing the crystal. In the case of the N9-Pan complex a 0.5 *M* solution was prepared in 100% DMSO and 1 µl of the ligand solution was added to the drop containing the crystal. In each case, the crystal was soaked for at least 16 h prior to flash-freezing for X-ray data collection.

2.4. Data collection, structure solution, refinement, modelling and validation

X-ray diffraction data were collected for the complexes of *Mt*PanK with pantothenol and N9-Pan using a MAR 345 image-plate mounted on a Rigaku RU-200 rotating-anode X-ray generator. X-ray data for the pantothenate complex were collected on a Bruker AXS Microstar Ultra II rotating-anode X-ray generator. The ligand-soaked crystals were flash-frozen at 100 K in a liquid-nitrogen stream produced by an Oxford Cryosystem and data were collected with an oscillation angle of 1°. The images recorded for the pantothenol and N9-Pan complexes were processed and scaled using *DENZO* and *SCALEPACK* from the *HKL* package (Otwinowski & Minor, 1997). For the pantothenate data set the programs *MOSFLM* and *SCALA* from the *CCP*4 suite were used (Winn *et al.*, 2011).

The intensity data were truncated to amplitudes using *TRUNCATE* from the *CCP*4 suite and the structures were solved by molecular replacement using the *Mt*PanK structure 2gev (Das *et al.*, 2006) as the search model. *Phaser* from the *CCP*4 suite was used for molecular replacement for the pantothenate complex, while *AMoRe* (Navaza, 1994) was used for the pantothenol and N9-Pan complexes. Initial refinement of all structures was performed using *CNS* (Brünger *et al.*, 1998). The structures were subjected to rigid-body refinement followed by positional refinement. Bound ligands were located using electron-density maps with Fourier coefficients $2F_o - F_c$ and $F_o - F_c$. The locations were further confirmed by calculating several simulated-annealing OMIT maps (with a starting temperature of 1000 K and a cooling rate of 50 K) during the course of refinement and iterative model building.

Iterative model building was carried out using the interactive graphics program *Coot* until convergence of R and R_{free} (Emsley & Cowtan, 2004). In all structures water molecules were built into the electron-density maps where peaks were visible at contours of at least 3σ in $F_o - F_c$ and 1σ in $2F_o - F_c$ electron-density maps. The topology and parameter files for the various ligands were generated using the *PRODRG* server (Schüttelkopf & van Aalten, 2004). The models were validated

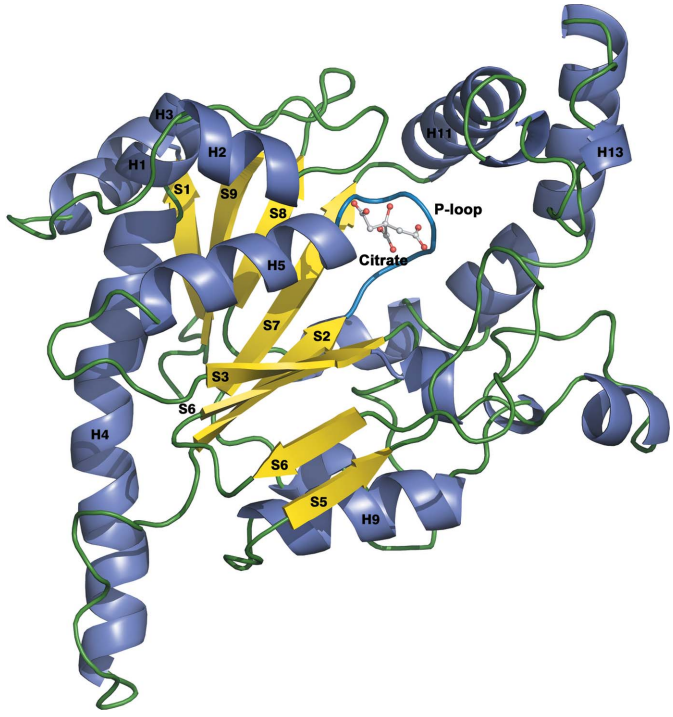

Figure 1
Overall structure of *Mt*PanK. The central seven-stranded β-sheet is depicted in yellow and the surrounding α-helices are shown in slate. The conserved P-loop is shown in sky blue and the bound citrate ion is shown in grey in a ball-and-stick representation.

using *PROCHECK* and *MolProbity* (Laskowski *et al.*, 1993; Davis *et al.*, 2007). Secondary structure was assigned using *DSSP* (Kabsch & Sander, 1983). Structural superpositions were made using *ALIGN* (Cohen, 1997). Interatomic distances were calculated using *CONTACT* from the *CCP*4 program suite (Winn *et al.*, 2011). For assigning hydrogen bonds, a distance of less than or equal to 3.6 Å between the donor (D) and the acceptor (A) atom and a D—H···A angle greater than 90° were used. Buried surface area was calculated using *NACCESS* (Hubbard & Thornton, 1996). The volume of the ligand-binding pocket was calculated using the *CASTp* server (Dundas *et al.*, 2006). All figures for molecular representation were prepared using *PyMOL* (DeLano, 2002). Modelling was performed using *ArgusLab* (Thompson, 2004) and *CNS* (Brünger *et al.*, 1998). The routine implemented in *CNS* was used for morphing (Krebs & Gerstein, 2000). Refinement parameters, together with data-collection statistics, are given in Table 1.

Table 1
Data-collection statistics and refinement parameters.

Values in parentheses are for the highest resolution shell.

Ligand	Pantothenate	Pantothenol	N9-Pan
Space group	$P3_121$	$P3_121$	$P3_121$
Unit-cell parameters (Å)	a = 103.39, c = 91.00	a = 103.64, c = 91.15	a = 103.84, c = 91.03
V_M (Å^3 Da^{-1})	3.81	4.02	3.84
Solvent content (%)	67.7	69.4	67.9
No. of subunits per asymmetric unit	1	1	1
Resolution (Å)	40.0–2.55 (2.69–2.55)	30.0–2.60 (2.69–2.60)	25.0–3.00 (3.11–3.00)
No. of measured reflections	92637	116253	43870
No. of unique reflections	18703 (2675)	17795 (1746)	11555 (1145)
Completeness (%)	99.9 (99.7)	99.8 (100.0)	98.9 (99.1)
R_{merge}†	7.8 (54.8)	7.2 (53.8)	12.7 (54.4)
$\langle I/\sigma(I)\rangle$	11.9 (2.3)	26.3 (3.7)	10.8 (2.7)
Multiplicity	5.0 (4.9)	6.5 (6.5)	3.8 (3.8)
Refinement and model statistics			
No. of reflections	18667	17768	11542
R factor (%)	22.0	20.7	20.4
R_{free}‡ (%)	24.9	23.3	26.0
No. of atoms in asymmetric unit			
Protein	2473	2462	2471
Ligand	28	27	37
Solvent/ions	246	297	245
R.m.s. deviations from ideal			
Bond lengths (Å)	0.006	0.006	0.009
Bond angles (°)	1.4	1.4	1.4
Ramachandran plot statistics§			
Most favoured region (%)	91.2	89.4	86.4
Additionally allowed region (%)	7.7	8.8	11.4
Genereously allowed region (%)	1.1	1.5	1.8
Disallowed region (%)	0	0.4	0.4

† $R_{merge} = \sum_{hkl}\sum_i |I_i(hkl) - \langle I(hkl)\rangle| / \sum_{hkl}\sum_i I_i(hkl)$, where $I_i(hkl)$ is the ith intensity measurement of a reflection, $\langle I(hkl)\rangle$ is the average intensity value of that reflection and the summation is over all measurements. ‡ 5% of the reflections were used for the R_{free} calculations. § Calculated for nonglycine and nonproline residues using *PROCHECK*.

3. Results

3.1. Overall features

*Mt*PanK has a mononucleotide-binding fold and belongs to the family of P-loop kinases, with its structure consisting of a central seven-stranded β-sheet flanked by α-helices (Fig. 1). Nucleotide binding in *Mt*PanK, like in other P-loop kinases, is accomplished through a conserved structural Walker A motif (G*XXXX*GKS/T). The conserved motif is part of a connecting loop between a β-strand and an α-helix and it wraps over the triphosphate tail of the nucleotide. The three crystal structures reported here have one ligand bound to each subunit. They belong to the same space group and have comparable unit-cell parameters.

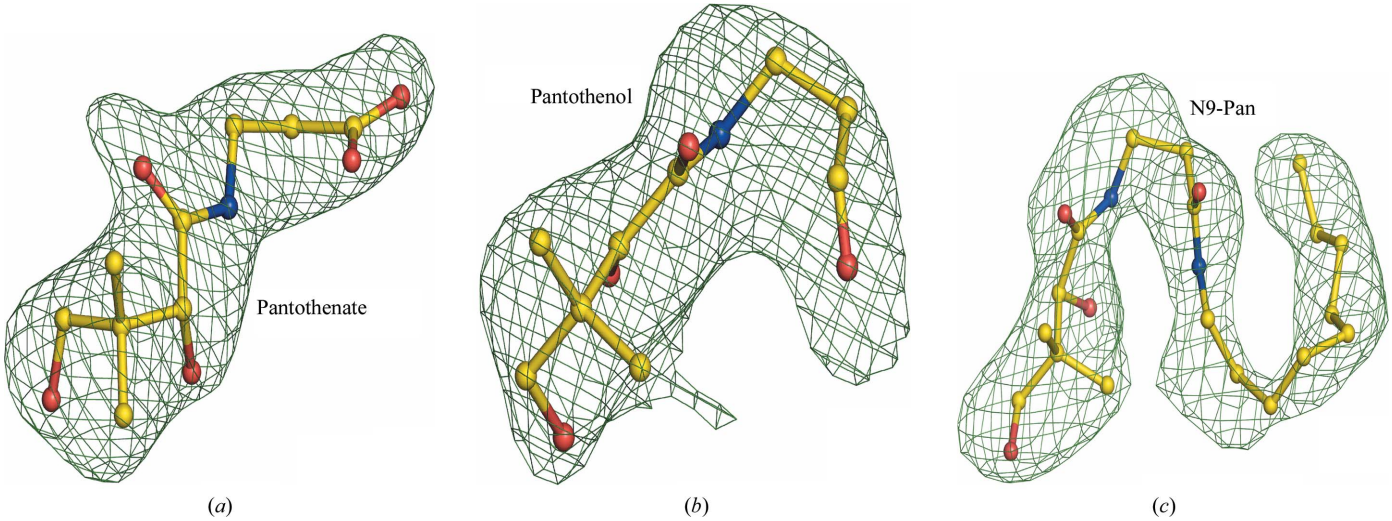

Figure 2
Simulated-annealing OMIT map with Fourier coefficients $F_o - F_c$ contoured at 5.0σ for ligands bound to *Mt*PanK in (*a*) the pantothenate binary complex, (*b*) the pantothenol binary complex and (*c*) the N9-Pan binary complex.

The first five residues in the three *Mt*PanK structures are disordered and the biologically relevant dimer is generated in each case through the crystallographic twofold axis. The protein molecules in the three complexes superpose with an overall r.m.s. deviation ranging from 0.26 to 0.32 Å when all 307 C^{α} positions are used. The ligands in the molecules could be unambiguously located in the active site (Fig. 2). In all three structures a citrate ion from the buffer binds to the P-loop through extensive hydrogen bonding, as in the crystal structure of unliganded *Mt*PanK. In addition, the binding site contains two glycerol molecules in the pantothenate complex and one in the pantothenol complex.

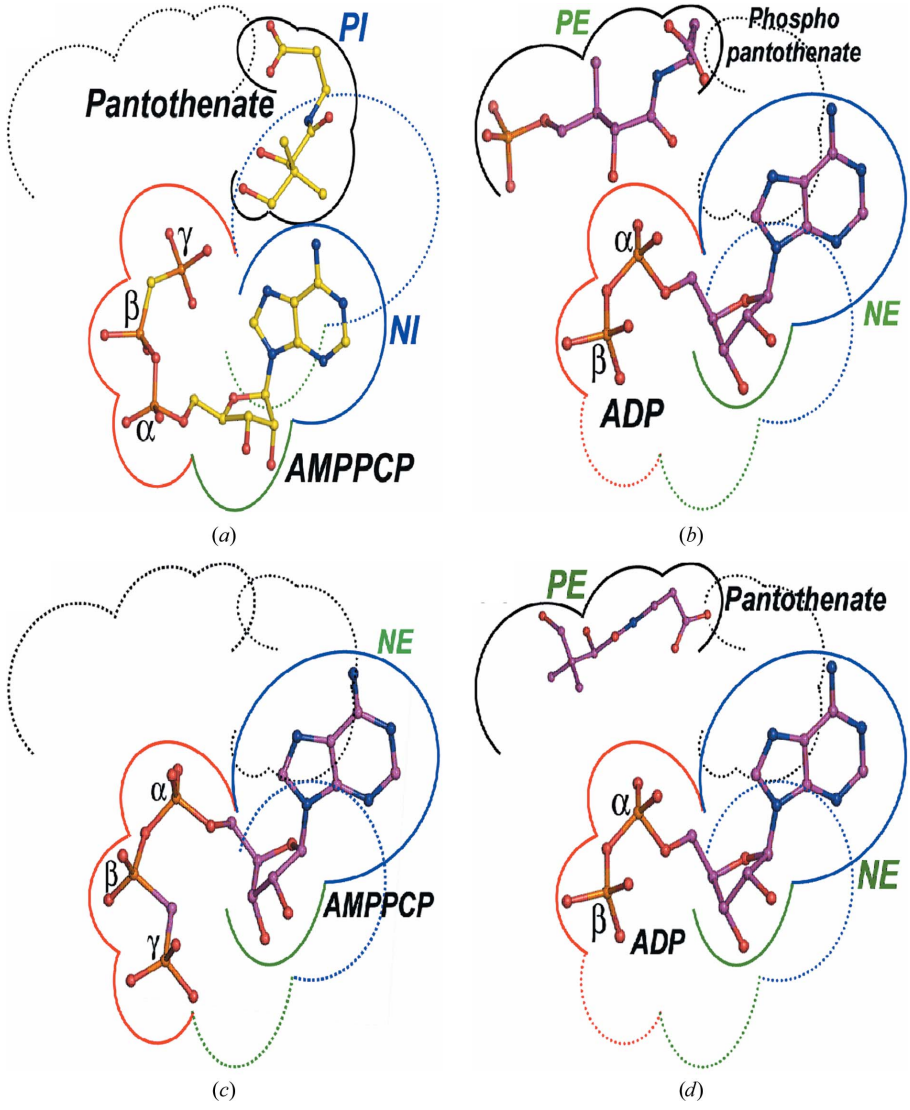

Figure 3
Overview of changes in ligand location during enzyme action in *Mt*PanK. Solid lines represent the ligand locations as seen in the crystal structures. Dotted lines represent vacant ligand-binding sites. (*a*) Initiation complex, (*b*) end complex (*c*) binary complex with AMPPCP and (*d*) ternary complex with ADP and pantothenate.

3.2. Natural locations and conformations of ligands

Previous studies had indicated that the movement of ligands involves four sites, as illustrated in Fig. 3. The locations of NTP and pantothenate in the initiation complex (Fig. 3*a*) are referred to as NI and PI and those of NDP and phosphopantothenate in the end complex as NE and PE (Fig. 3*b*). The NTP at NI exists in the closed conformation, with the γ-phosphate pointing to the hydroxyl group of the pantothenate located at PI in a closed conformation. After phosphorylation, NDP assumes an extended conformation and shifts to location NE as in the end complex. The shift in the nucleotide after phosphorylation is such that the base now moves into a region that is occupied by pantothenate in the initiation complex but vacated on phosphorylation. NDPs retain their position at NE in their binary complexes with *Mt*PanK and also in their ternary complexes involving pantothenate. Interestingly, AMPPCP and GMPPCP also have extended conformations and are located at NE in their binary complexes with *Mt*PanK (Fig. 3*c*). Thus, the conformation and location of AMPPCP and GMPPCP in their binary complexes are similar to those of ADP and GDP in all their complexes, including ternary complexes involving pantothenate (Fig. 3*d*). The nucleoside triphosphates assume a closed conformation and move to NI in the presence of pantothenate. Thus, the crystal structures analyzed so far define the natural conformations and locations of the nucleotides in their binary complexes and also those in the presence of pantothenate.

The residues affected by the binding of the ligand in the three complexes reported here are listed in Table 2 along with those affected by the presence of pantothenate in the ATP initiation complex (at PI) and the pantothenate moiety in the ATP end complex (at PE). Clearly, pantothenate and pantothenol occupy PE, while N9-Pan spans PI and PE. A superposition of the ligands and a few surrounding residues in the three complexes is shown in Fig. 4.

Pantothenate, pantothenol and the pantothenamide moiety of N9-Pan located at PE superpose well onto one another, while the long alkyl tail of N9-Pan is located at NI. There is some departure from the common location at the carboxyl end of pantothenate resulting from the replacement of the carboxyl by a hydroxyl or an amide in pantothenol and N9-Pan, respectively. However, the locations of the three ligands, except for the alkyl tail of N9-Pan, are essentially the same

Table 2
List of residues in *Mt*PanK complexes that exhibit changes in their accessible surface area upon binding of pantothenate or pantothenate analogues.

Pantothenate in ATP initiation complex	Pantothenate moiety of phosphopantothenate in ATP end complex	Binary complex with pantothenate	Binary complex with pantothenol	Binary complex with N9-Pan
Val99	Val99	Val99	Val99	Val99
—	Asp129	Asp129	Asp129	Asp129
—	Leu132	Leu132	Leu132	Leu132
—	—	His145	—	—
—	Lys147	Lys147	Lys147	Lys147
—	Gly148	Gly148	Gly148	Gly148
—	Tyr153	Tyr153	Tyr153	Tyr153
—	Tyr177	Tyr177	Tyr177	Tyr177
—	His179	His179	His179	His179
Tyr182	Tyr182	Tyr182	Tyr182	Tyr182
—	Leu203	Leu203	Leu203	Leu203
Tyr235	Tyr235	—	Tyr235	Tyr235
Arg238	—	—	—	Arg238
Phe239	—	—	—	Phe239
Met242	—	—	—	Met242
Phe247	—	—	—	Phe247
Phe254	Phe254	Phe254	—	Phe254
Tyr257	—	—	—	Tyr257
Ile272	Ile272	Ile272	Ile272	Ile272
Ile276	Ile276	Ile276	Ile276	Ile276
Asn277	Asn277	Asn277	Asn277	Asn277

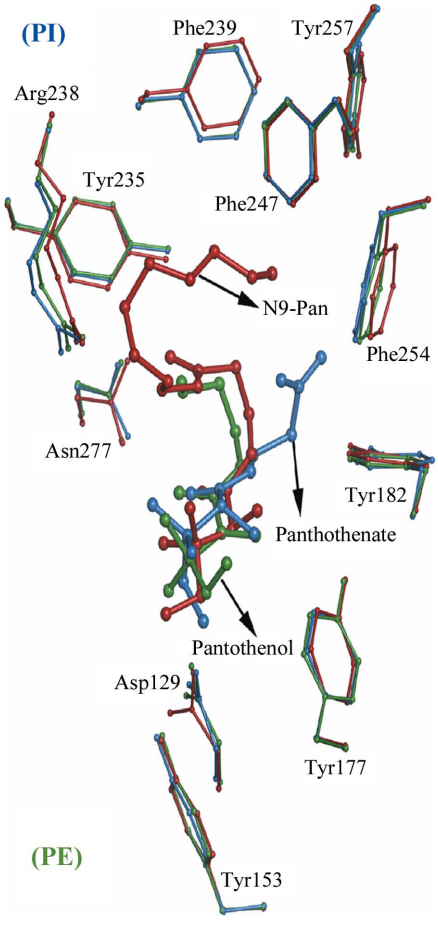

Figure 4
Natural location of pantothenate and its derivatives in *Mt*PanK. Pantothenate, pantothenol and N9-Pan together with the residues which make up their binding sites are shown in blue, green and red, respectively, in ball-and-stick representation.

and correspond to the location of phosphopantothenate in the end complex, with some changes resulting from the absence of the phosphoryl group, and that of pantothenate in the ternary complexes involving NDP and pantothenate. Thus, the three complexes establish that the natural location of pantothenate is at PE. The vacant PI site in the pantothenate complex is occupied by two glycerol molecules. The altered conformation resulting from the replacement of the carboxyl group in pantothenate by a hydroxyl group in pantothenol is such that the hydroxyl group replaces one of the glycerol molecules in the pantothenol complex. Both the glycerol molecules are replaced by the alkyl chain in the N9-Pan complex.

Pantothenate can assume a variety of conformations (Salunke & Vijayan, 1984). That in the binary complex is substantially extended except at the carboxyl end. The conformation is such that the carboxyl group forms a hydrogen bond to the hydroxyl group of Tyr182. With the replacement of the carboxyl group by a hydroxyl group or an amide group in pantothenol and N9-Pan, this hydrogen bond is abolished and the bend in this region of the molecule becomes more pronounced. The interactions of pantothenate with *Mt*PanK in the binary complex are substantially nonpolar. In addition to the hydrogen bond referred to above, the central hydroxyl group is involved in a water-mediated interaction with the side-chain hydroxyl of Tyr177. The interaction of pantothenol and N9-Pan with *Mt*PanK is also substantially nonpolar. The only hydrogen bond in the pantothenol complex is between its central carbonyl group and the side-chain NH group of Asn277. In the N9-Pan complex, the carbonyl O atom of the amide group resulting from derivatization forms hydrogen bonds to the side-chain NH of Asn277 and the hydroxyl group of Tyr235.

It is interesting to compare the locations of the ligands with that of pantothenate in *Ec*PanK, as revealed by X-ray analysis of its ternary complex with ADP and pantothenate, and the modelled location of N5-Pan derived from the structure of the complex (Ivey *et al.*, 2004). Pantothenate and the pantothenamide component of N5-Pan/N9-Pan are located at PE in the *Ec*PanK and *Mt*PanK complexes. As in the case of the alkyl chain of N9-Pan in the *Mt*PanK complex, that of N5-Pan in the modelled *Ec*PanK complex also resides at PI. The hydrophobic residues involved in lining the alkyl chain in the *Ec*PanK complex, Phe239, Phe242 (Met in *Mt*PanK), Phe254 and Tyr257 (residue numbering as in *Mt*PanK), are also involved in lining the chain in the *Mt*PanK–N-Pan complex. In addition, Tyr235 and Phe247 also line the alkyl chain in the latter. The β-mercaptoethanolamine tail of CoA binds in the same pocket in the *Ec*PanK–CoA complex (Yun *et al.*, 2000).

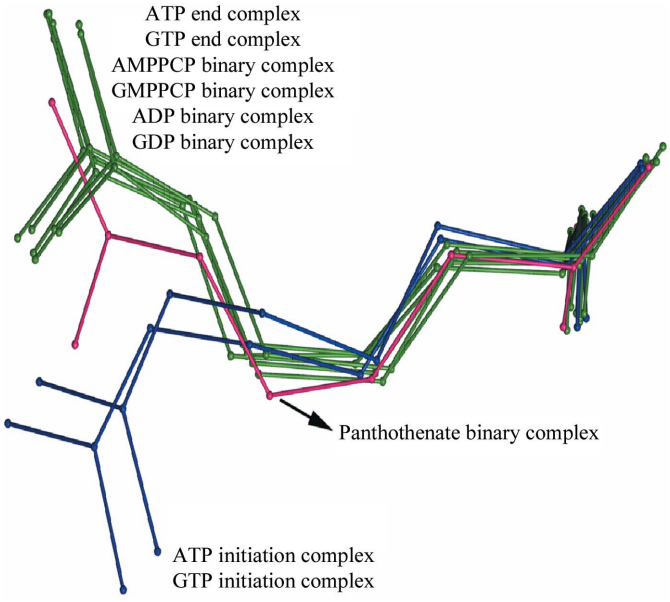

Figure 5
The side-chain conformations of Arg238 in different *Mt*PanK structures. The side-chain conformations of this residue cluster into two distinct groups. The first group (blue) is made up by the ATP and GTP initiation complexes. The second group is made up by the ADP and GDP end-complex structures along with the binary-complex structures involving trinucleotides or dinucleotides. The conformation of Arg238 in the pantothenate binary complex (pink) roughly falls into the second cluster.

In the corresponding *Mt*PanK complex, the tail extends presumably on account of reaction with β-mercaptoethanol in the crystallization medium (Das *et al.*, 2006). The extended tail also comfortably fits in the pocket.

In the presence of NTPPCP or NDP the PI site is not accessible to pantothenate or its analogues as the site is partially occupied by the nucleotide base. However, as the two binary complexes indicate, pantothenate and pantothenol do not bind at PI even in the absence of nucleotides. In the binary complex of N9-Pan, the pantothenamide component remains at PE and only the alkyl chain occupies PI. On close examination, it appears that the difference in the conformation of Arg238 in the initiation complex and in the other structures could be a reason for the inability of pantothenate, pantothenol and the pantothenamide component of N9-Pan to bind at PI even in the absence of nucleotides. The conformation of the side chain in all of the structures except those of the initiation complexes is similar to that in the binary complexes reported here (Fig. 5). The consequence of the difference in conformation becomes immediately obvious on examining Fig. 6, which shows a van der Waals representation of PI in the ATP initiation complex and the *Mt*PanK–pantothenate structure. Pantothenate neatly fits in the binding site in the former. However, the hydroxyl end of pantothenate would make steric clashes with the arginyl side chain in the altered conformation in the latter. Thus, pantothenate cannot readily

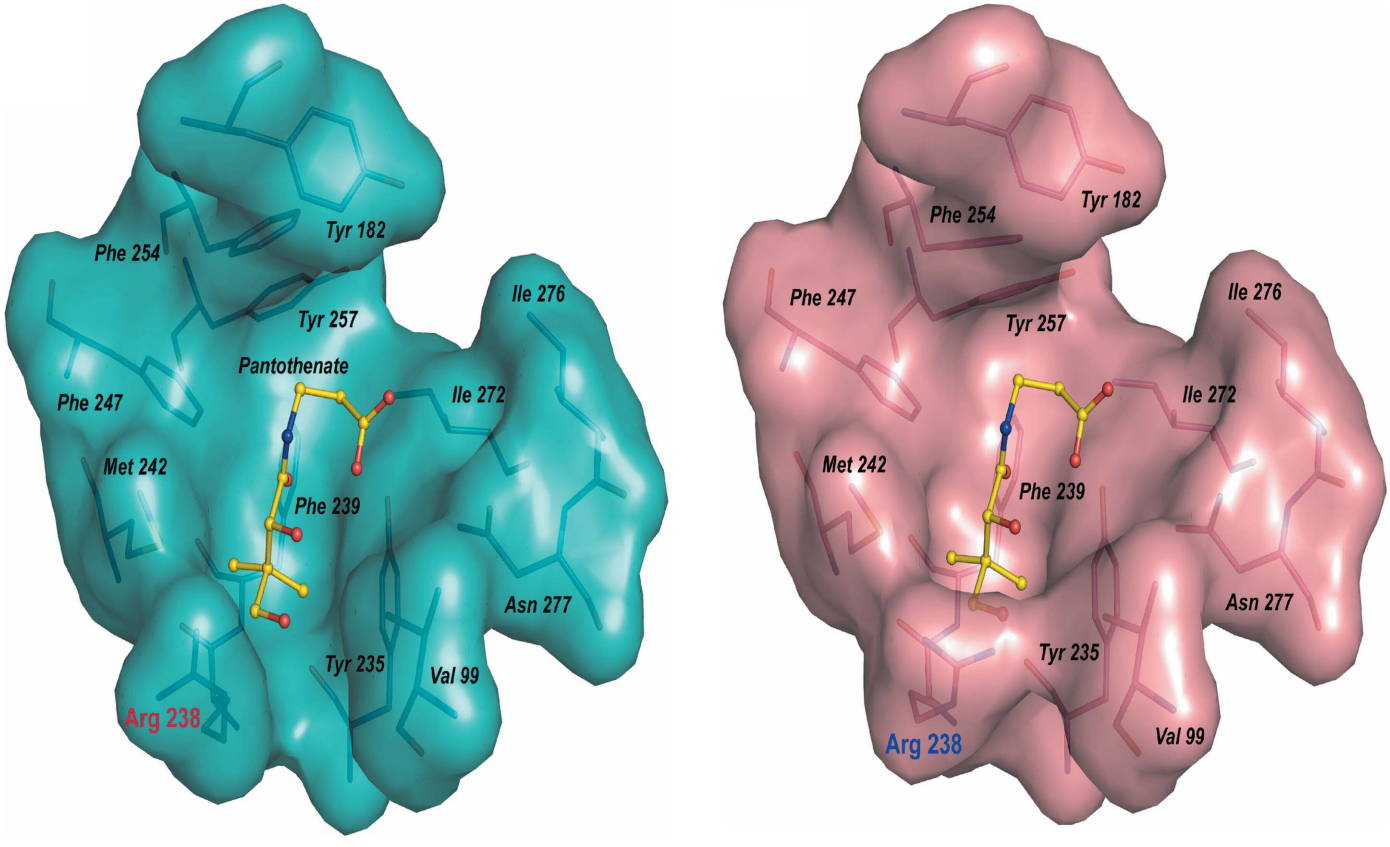

(*a*) (*b*)

Figure 6
van der Waals surface representation of the PI site in (*a*) the ATP initiation complex and (*b*) the pantothenate binary complex. The location of pantothenate as in the initiation complex is also shown in (*b*).

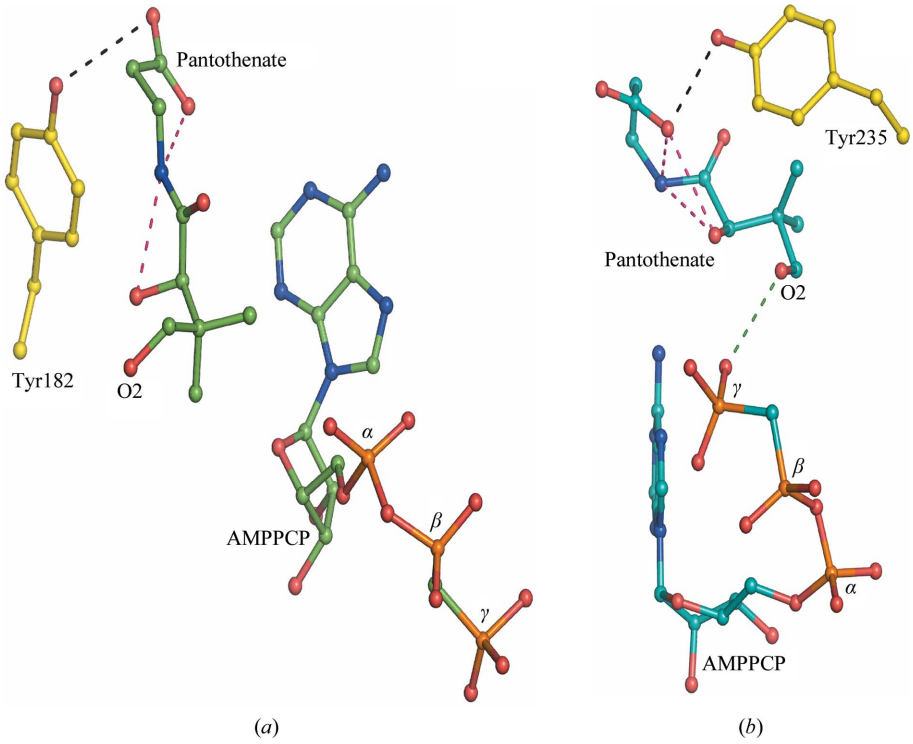

Figure 7
Mutual disposition of AMPPCP and pantothenate in (*a*) their natural locations and (*b*) the ATP initiation complex. Dashed lines in black, pink and green represent protein–pantothenate, intra-pantothenate and AMPPCP–pantothenate hydrogen bonds.

bind at PI except in the initiation complex. The same is true of pantothenol and the pantothenamide component of N9-Pan.

3.3. Structural rationale for the change in the location and the conformation of ligands

The natural locations and conformations of AMPPCP and pantothenate observed in their binary complexes are illustrated in Fig. 7(*a*). Phosphorylation obviously cannot take place with this mutual disposition as the distance between the γ-phosphate and the terminal pantothenyl hydroxyl group (O2) is as large as 12 Å. The locations and conformations of the vitamin and the NTP in the productive initiation complex are shown in Fig. 7(*b*). The mutual disposition of the two ligands is now appropriate for phosphorylation.

It has been demonstrated that pantothenol is also phosphorylated by the enzyme (Kumar *et al.*, 2007). An experiment involving N9-Pan and radiolabelled ATP showed that *Mt*PanK can successfully phosphorylate N9-Pan and the amount of phosphorylated product formed is directly proportional to the concentration of N9-Pan used (Fig. 8). Pantothenol can be clearly accommodated at PI when the site is free and accessible, as in the initiation complex. The situation is not obvious in the case of N9-Pan. In order to explore this, the pantothenamide moiety was superposed on the pantothenate in the initiation complex. The alkyl tail then almost naturally fits into the PE site. Thus, N9-Pan also can bind to the enzyme in the productive mode. Phosphorylated pantothenol can also readily occupy the position of phosphopantothenate in the end complex. Despite the long alkyl tail in the ligand, a model of the end complex of *Mt*PanK with N9-Pan could be constructed with the phosphorylated pantothenamide moiety superposing on phosphopantothenate in the *Mt*PanK–ADP–phosphopantothenate end complex. Thus, pantothenol and N9-Pan can form initiation and end complexes of the type formed by pantothenate, with the common regions of the three ligands occupying nearly the same locations in both sets of complexes. The question is why and how the system shifts from the situation illustrated in relation to pantothenate in Fig. 7(*a*) to that described in Fig. 7(*b*). Modelling indicates that the two situations are also similar in relation to the other two ligands.

The surface area of the enzyme buried on complexation in the initiation complex corresponding to the situation represented in Fig. 7(*b*) was estimated using the crystal structure involving pantothenate (Chetnani *et al.*, 2009). Similar estimations were made using comparable models involving pantothenol and N9-Pan instead of pantothenate. In the situation corresponding to Fig. 7(*a*) the buried surface area was obtained by addition of the area buried in the binary complex with AMPPCP and that buried in the binary complexes with pantothenate, pantothenol and N9-Pan. In all the three cases, the surface areas buried in the two situations were comparable. The same is true for the number of protein–ligand hydrogen bonds in the two situations in each case. However, a hydrogen bond between the two ligands (Fig. 7*b*) exists in the initiation complex involving pantothenate. The same hydrogen bond can also exist in the complexes involving pantothenol and N9-Pan, as changes occur only at the carboxyl end when pantothenate is replaced by pantothenol or N9-Pan. Furthermore, the number of internal hydrogen bonds in panthothenate is higher in the initiation complex, where it has a closed conformation, than when it is at its natural location. The same turns out to be true when pantothenol and N9-Pan in their modelled initiation complexes are compared with their respective binary complexes. Thus, the situation represented by Fig. 7(*b*) appears to be energetically preferred. In the absence of the other ligand, the arrangement found in the appropriate binary complexes is preferred. In the presence of both ligands, the arrangement found in the initiation complexes is preferred.

Once pantothenate (or its analogues) is phosphorylated, the ligands move to the locations found in the end complex(es). The ligands also assume somewhat extended conformations.

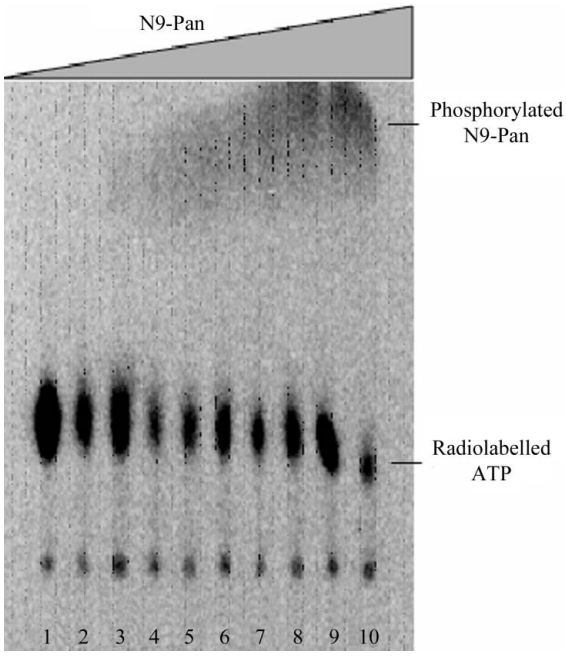

Figure 8
Phosphorylation of N9-Pan by *Mt*PanK. The concentration of N9-Pan was increased sequentially in lanes 1–10 and the amount of phosphorylated N9-Pan formed was directly proportional to its starting concentration in the reaction mixture.

The structural rationale for these changes has previously been discussed (Chetnani *et al.*, 2009). Incidentally, the locations and conformations of ligands observed in the end complex(es) are similar to those in the respective binary complexes and thus correspond to their natural locations and conformations. Therefore, the path traversed by the ligands, accompanied by changes in conformation, when moving from their natural locations to those in the initiation complex is likely to be similar to the reverse of the path followed when moving from the initiation complex to the end complex. Morphing between different complexes (Krebs & Gerstein, 2000) indicates that this is indeed the case, in addition to demonstrating that pantothenate, pantothenol and N9-Pan could have roughly the same trajectories during movement from one location to another.

4. Discussion

The results reported here complete the structural characterization of the interactions of *Mt*PanK with AMPPCP, ADP, GMPPCP, GDP, pantothenate, CoA and phosphopantothenate in binary and ternary complexes. The binary complexes are of interest as they define the natural location of each ligand unaffected by the presence of one or another of the remaining ligands. The ternary complexes provide information on the state of the system, particularly at the beginning and end of the catalytic process. The binary complexes of pantothenol and N9-Pan presented here together with that of pantothenate provide comprehensive information on their interactions with *Mt*PanK. This information helps in exploring the geometrical features of phosphorylation of the two substrate analogues based on the features associated with the phosphorylation of pantothenate.

*Mt*PanK provides a rare example of an enzyme with equal specificity for ATP and GTP. The structural basis of this dual specificity, which is in contrast to the higher specificity of *Ec*PanK for ATP, has been clearly established from the relevant crystal structures (Chetnani *et al.*, 2010). *Mt*PanK does not exhibit structural changes of the type exhibited by *Ec*PanK when interacting with nucleoside diphosphates and triphosphates. Again unlike in the case of *Ec*PanK, ligands exhibit substantial changes in location and conformation during catalysis by *Mt*PanK, irrespective of whether ATP or GTP is the substrate. ATP (or GTP) perhaps initially interacts with the enzyme in a folded conformation, but it appears to assume an extended conformation at a somewhat different location, as revealed by the structures of the binary complexes of the enzyme with AMPPCP and GMPPCP. The natural location of pantothenate, in which it exists in a somewhat extended conformation, could be clearly delineated in the *Mt*PanK–pantothenate binary complex. When a nucleotide triphosphate and pantothenate simultaneously interact with the enzyme, the location and the conformation of both change, as revealed by the structures of the initiation complexes. The new location and conformation are such as to facilitate phosphoryl transfer in terms of the orientation and proximity of the donating and accepting groups. Once the transfer is over, pantothenate bearing the phosphoryl group returns to its natural location; the nucleoside diphosphate in the extended conformation shifts to the location of the nucleotide triphosphates found in their binary complexes, as can be seen from the structure of the end complexes.

As mentioned in a previous communication (Chetnani *et al.*, 2009), structural features indicate that although the mechanism of *Mt*PanK is predominantly associative, as in the case of *Ec*PanK, the dissociative component appears to be greater in *Mt*PanK than in *Ec*PanK. Kinetic analysis had previously suggested a sequential mechanism for *Ec*PanK with ATP binding first and pantothenate second (Song & Jackowski, 1994). The structural changes in the enzyme associated with ligand binding appear to be in consonance with this suggestion (Yun *et al.*, 2000; Ivey *et al.*, 2004). In the case of *Mt*PanK, the kinetic analysis reported to date (Kumar *et al.*, 2007) does not provide direct evidence for a sequential ordered mechanism. Therefore, whether ATP binds first to the enzyme as in the case of *Ec*PanK remains an open question. However, it is interesting to note in this context that unlike *Ec*PanK, *Mt*PanK exhibits no significant structural changes upon ligand binding. Ligands undergo changes in location (and conformation) during enzyme action, but they occur within a substantially rigid binding region.

The crystal structures of the binary complexes involving pantothenol and N9-Pan reported here and the modelling studies involving them lend additional support to the conclusions derived from the previous extensive studies involving pantothenate. The work involving N9-Pan is particularly

interesting as *N*-alkylpanthotanamides have received considerable attention as inhibitors of fatty-acid synthesis and possibly CoA synthesis (Strauss & Begley, 2002; Ivey *et al.*, 2004; Thomas & Cronan, 2010). Furthermore, unlike pantothenol, N9-Pan is a much larger ligand than pantothenate on account of the additional long alkyl chain that is present. Crystallographic, modelling and morphing studies clearly indicate that despite the additional bulk of N9-Pan, it and pantothenate can behave in a similar manner, including the change in location and conformation. The results of modelling studies on the interaction of N5-Pan and N7-Pan with *Ec*PanK (Ivey *et al.*, 2004) are consistent with this observation. Biochemical results on the phosphorylation of *N*-alkylpantothenamides by *Mt*PanK reported here and those involving *Ec*PanK reported previously (Strauss & Begley, 2002; Ivey *et al.*, 2004) suggest that these pantothenamides are good substrates of PanK. There is no evidence to suggest that they are inhibitors of PanK. If they inhibit CoA synthesis (Thomas & Cronan, 2010), the site of inhibition is likely to be further down the synthetic pathway.

The series of *Mt*PanK structures reported previously (Chetnani *et al.*, 2009, 2010), together with the structures of the binary complex of pantothenate reported here, provide a reasonably comprehensive picture of the natural locations and conformations of nucleoside diphosphates and triphosphates and pantothenate in the enzyme, and the locations and conformations of the ligands in the ternary initiation and end complexes. The structures also give some indication of the rationale for the movement and conformational changes exhibited by the ligands during catalysis. The crystal structures of the binary complexes of pantothenol and N9-Pan and modelling studies suggest that the movements involved in the phosphorylation of these ligands and other *N*-alkylpantothenamides by PanK could be the same as those involved in the phosphorylation of pantothenate. The investigations presented here, particularly those involving N9-Pan, provide further insights into the catalytic action of *Mt*PanK and the nature of the binding site which could be useful in inhibitor design with the objective of possible drug development in view of the essential nature of the enzyme.

The data sets used in the present work were collected at the X-ray facility for Structural Biology at the Institute, supported by the Department of Science and Technology (DST). In addition to the in-house facilities, those at the Bioinformatics Centre and Graphics facility, both supported by the Department of Biotechnology (DBT), were also used for computations. Financial support from DBT is acknowledged. KVA is a CSIR Junior Fellow. MV is a DAE Homi Bhabha Professor.

References

Brünger, A. T., Adams, P. D., Clore, G. M., DeLano, W. L., Gros, P., Grosse-Kunstleve, R. W., Jiang, J.-S., Kuszewski, J., Nilges, M., Pannu, N. S., Read, R. J., Rice, L. M., Simonson, T. & Warren, G. L. (1998). *Acta Cryst.* D**54**, 905–921.
Chetnani, B., Das, S., Kumar, P., Surolia, A. & Vijayan, M. (2009). *Acta Cryst.* D**65**, 312–325.
Chetnani, B., Kumar, P., Surolia, A. & Vijayan, M. (2010). *J. Mol. Biol.* **400**, 171–185.
Cohen, G. E. (1997). *J. Appl. Cryst.* **30**, 1160–1161.
Das, S., Kumar, P., Bhor, V., Surolia, A. & Vijayan, M. (2006). *Acta Cryst.* D**62**, 628–638.
Davis, I. W., Leaver-Fay, A., Chen, V. B., Block, J. N., Kapral, G. J., Wang, X., Murray, L. W., Arendall, W. B., Snoeyink, J., Richardson, J. S. & Richardson, D. C. (2007). *Nucleic Acids Res.* **35**, W375–W383.
DeLano, W. L. (2002). *PyMOL*. http://www.pymol.org.
Dundas, J., Ouyang, Z., Tseng, J., Binkowski, A., Turpaz, Y. & Liang, J. (2006). *Nucleic Acids Res.* **34**, W116–W118.
Emsley, P. & Cowtan, K. (2004). *Acta Cryst.* D**60**, 2126–2132.
Hubbard, S. J. & Thornton, J. M. (1996). *NACCESS Computer Program*. Department of Biochemistry and Molecular Biology, University College London.
Ivey, R. A., Zhang, Y.-M., Virga, K. G., Hevener, K., Lee, R. E., Rock, C. O., Jackowski, S. & Park, H.-W. (2004). *J. Biol. Chem.* **279**, 35622–35629.
Kabsch, W. & Sander, C. (1983). *Biopolymers*, **22**, 2577–2637.
Krebs, W. G. & Gerstein, M. (2000). *Nucleic Acids Res.* **28**, 1665–1675.
Krishna, R., Prabu, J. R., Manjunath, G. P., Datta, S., Chandra, N. R., Muniyappa, K. & Vijayan, M. (2007). *J. Mol. Biol.* **367**, 1130–1144.
Kumar, P., Chhibber, M. & Surolia, A. (2007). *Biochem. Biophys. Res. Commun.* **361**, 903–909.
Laskowski, R. A., Moss, D. S. & Thornton, J. M. (1993). *J. Mol. Biol.* **231**, 1049–1067.
Leonardi, R., Zhang, Y.-M., Rock, C. O. & Jackowski, S. (2005). *Prog. Lipid Res.* **44**, 125–153.
Navaza, J. (1994). *Acta Cryst.* A**50**, 157–163.
Otwinowski, Z. & Minor, W. (1997). *Methods Enzymol.* **276**, 307–326.
Prabu, J. R., Thamotharan, S., Khanduja, J. S., Chandra, N. R., Muniyappa, K. & Vijayan, M. (2009). *Biochim. Biophys. Acta*, **1794**, 1001–1009.
Roy, S., Saraswathi, R., Chatterji, D. & Vijayan, M. (2008). *J. Mol. Biol.* **375**, 948–959.
Salunke, D. M. & Vijayan, M. (1984). *Biochim. Biophys. Acta*, **798**, 180–186.
Schüttelkopf, A. W. & van Aalten, D. M. F. (2004). *Acta Cryst.* D**60**, 1355–1363.
Selvaraj, M., Roy, S., Singh, N. S., Sangeetha, R., Varshney, U. & Vijayan, M. (2007). *J. Mol. Biol.* **372**, 186–193.
Song, W. J. & Jackowski, S. (1994). *J. Biol. Chem.* **269**, 27051–27058.
Spry, C., Kirk, K. & Saliba, K. J. (2008). *FEMS Microbiol. Rev.* **32**, 56–106.
Strauss, E. & Begley, T. P. (2002). *J. Biol. Chem.* **277**, 48205–48209.
Thomas, J. & Cronan, J. E. (2010). *Antimicrob. Agents Chemother.* **54**, 1374–1377.
Thompson, M. A. (2004). *ArgusLab*. Planaria Software LLC, Seattle, Washington, USA. http://www.arguslab.com.
Vijayan, M. (2005). *Tuberculosis*, **85**, 357–366.
Winn, M. D. *et al.* (2011). *Acta Cryst.* D**67**, 235–242.
Yun, M., Park, C.-G., Kim, J.-Y., Rock, C. O., Jackowski, S. & Park, H.-W. (2000). *J. Biol. Chem.* **275**, 28093–28099.
Zhang, Y.-M., Frank, M. W., Virga, K. G., Lee, R. E., Rock, C. O. & Jackowski, S. (2004). *J. Biol. Chem.* **279**, 50969–50975.